Nutrition 67–68 (2019) 110557

Contents lists available at ScienceDirect

Nutrition

journal homepage: www.nutritionjrnl.com

Basic nutritional investigation

Proteome modifications of gut microbiota in mice with activity-based anorexia and starvation: Role in ATP production

Jonathan Breton P.hD. [a,b,c,*], Romain Legrand P.hD. [a,b], Najate Achamrah M.D., P.hD. [a,b,c], Philippe Chan P.hD. [b,d], Jean Luc do Rego P.hD. [b,e], Jean Claude do Rego P.hD. [b,e], Moïse Coëffier P.hD. [a,b,c], Pierre Déchelotte M.D., P.hD. [a,b,c], Sergueï O. Fetissov M.D., P.hD. [a,b,*]

[a] Normandie University, UNIROUEN, Nutrition, Gut and Brain Laboratory Rouen, France
[b] Normandie University, UNIROUEN, Institute for Research and Innovation in Biomedicine (IRIB), Rouen, France
[c] Nutrition Department, Rouen University Hospital, Rouen, France
[d] Normandie University, UNIROUEN, PISSARO Proteomic Platform, Mont-Saint-Aignan, France
[e] Normandie University, UNIROUEN, Animal Behavior Platform SCAC, Rouen, France

ARTICLE INFO

Article History:
Received 4 March 2019
Received in revised form 4 July 2019
Accepted 4 July 2019

Keywords:
Gut–brain axis
Microbiota
ATP
Acetate
Eating disorders
Anorexia nervosa
Activity-based anorexia

ABSTRACT

Objective: Activity-based anorexia (ABA) in rodents is a behavioral model of anorexia nervosa, characterized by negative energy balance, hyperactivity, and dysbiosis of gut microbiota. Gut bacteria are known to produce energy substrates including adenosine triphosphate (ATP) and acetate. The aim of this study was to determine whether ABA alters the proteome of gut microbiota relevant to ATP and acetate production.
Methods: The ABA was developed in male mice and compared with food-restricted and ad libitum–fed conditions. Proteomic analysis of feces was performed using the two-dimentional gel electrophoresis and mass spectrometry. The in vitro ATP-producing capacity of proteins extracted from feces was assayed.
Results: Increased levels of the phosphoglycerate kinase, an ATP-producing glycolytic enzyme, was detected in feces of food-restricted mice and this enzyme was further increased in the ABA group. Starvation also upregulated several other proteins synthetized by order Clostridiales including *Clostridiaceae* and *Lachnospiraceae* families. No significant differences in the in vitro ATP-producing capacity by bacterial proteins from ABA, food-restricted, and ad libitum–fed control mice were found. However, plasma levels of acetate strongly tended to be increased in the activity groups including ABA mice.
Conclusion: The data revealed that starvation in food-restricted and ABA mice induced proteome modification in gut bacteria favoring ATP production mainly by the order *Clostridiales.* However, this did not result in increased total ATP-production capacity by gut microbiota. These changes can be interpreted as an adaptation of specific gut bacteria to the host malnutrition beneficial for host survival.

Introduction

Anorexia nervosa (AN) is a form of eating disorder (ED) characterized by low food intake and for a subtype of patients, by hyperactivity leading to the negative energy balance and progressive loss of body weight [1]. Although the exact pathophysiologic mechanisms of AN and EDs remain unknown, gut microbiota appeared recently to be an important participant in the mechanisms regulating host appetite and feeding behavior as well as other functions involving the gut–brain axis [2–4]. Several studies in patients with AN reported the presence of gut microbiota dysbioses [5–10]. However, the significance of the reported modifications of gut bacterial composition to the pathophysiology of AN remains obscure [11–15] and may also non-specifically reflect the host starvation [16]. Host starvation and negative energy balance imposed to microbiota may effect the energy metabolism of gut bacteria, which are actively involved in both energy consumption, necessary for bacterial multiplication, as well as in energy production used by both bacteria and the host [2,17]. In fact, gut bacteria are a major source of several energy substrates in

This work was supported by the European Union and the Normandie Regional Council. Europe is involved in the Normandy with European Regional Development Fund (ERDF). SOF conceived of and designed the study. SOF and JB wrote the manuscript. JB contributed to the study design, performed the experiments, analyzed the data, and created the figures. RL and NA assisted with the experiments. PC performed the mass spectrometry analysis. MC and PD contributed to the study design. SOF is a co-founder and consultant of TargEDys, SA. PD is a co-founder of TargEDys, SA. The remaining authors have no conflicts of interest to declare.
* Corresponding authors: Tel.: + 332 35 14 82 40; Fax: +332 35 14 82 26; Tel.: + 332 35 14 61 93; Fax: +332 35 14 69 46.
E-mail addresses: Jonathan.breton1@univ-rouen.fr (J. Breton), Serguei.Fetissov@univ-rouen.fr (S.O. Fetissov).

https://doi.org/10.1016/j.nut.2019.110557
0899-9007/

the body including adenosine triphosphate (ATP) and short-chain fatty acids (SCFAs), such as acetate and butyrate [18,19]. Moreover, we previously demonstrated that proteins extracted from *Escherichia coli* dose-dependently catalyzed ATP production from various nutritional sources and influenced feeding behavior in rats and mice [20].

Activity-based anorexia (ABA) in rodents is a behavioral model of AN sharing the features of negative energy balance and hyperactivity. The relationship between the running wheel and the progressive limitation of food (from 6 h of free access at day 6 to 3 h at day 9; Fig. 1A) leads to the ABA phenotype. In fact, under the imposed restricted feeding schedule, rats and mice engage themselves in physical activity instead of feeding resulting in a "voluntary" decrease in food intake and progressive loss of body weight [21,22]. In addition to this central aspect in AN diagnosis, ABA rodents also share many similarities with patients, both physiologically (hypothermia [23–25], anhedonia [26,27], and increased susceptibility in younger rodents [28,29]) and behaviorally (females exercise more than males [30–32]). However, despite these well-described features, a complete neurocognitive assessment is needed to better characterize the model [33].

Dysbiosis of gut microbiota has been reported in ABA rats, which may share some modifications of gut microbiota found in patients with AN [34]. It is presently unclear whether the observed changes of gut bacterial composition in AN and ABA may alter energy substrate production capacity by gut bacteria toward catabolic or anabolic processes, which may indicate a pathologic or physiologic effect of gut microbiota on the host energy balance, respectively.

In the present study, we used the ABA model in mice to analyze the proteome of fecal microbiota for its relevance to ATP production. For this purpose, we compared fecal-extracted proteins between ABA, food-restricted, and ad libitum-fed groups of mice using two-dimensional (2-D) gel electrophoresis followed by mass spectrometry and by their in vitro capacity to catalyze ATP production from a mixed nutrient source of the Müeller-Hinton (MH) medium.

Material and methods

Animals

Animal care and experimentation complied with both French and European Community regulations (Official Journal of the European Community L 358, December 18, 1986), and MC was authorized by the French government to use animal models. Male C57 Bl/6 mice (Elevage Janvier, Le Genest St Isle, France) were acclimatized in individual cages at 23°C over a 7-d period. During this period and throughout the entire experiment, the 12-h light/dark cycle was inverted (dark phase: 0930 to 2130). At day (D) 1 of the experiment, mice were randomized into four groups depending on body weight: ABA (n = 8), feeding-time restriction (FTR; n = 8), ad libitum-fed controls with physical activity (CTPA; n = 8) and without (CT; n = 8) as previously described [35]. ABA and CTPA mice were placed in individual cages with an activity wheel operated by RunningWheel software (Intellibio, France). Wheel activity was continuously recorded. FTR and control mice were placed in individual cages

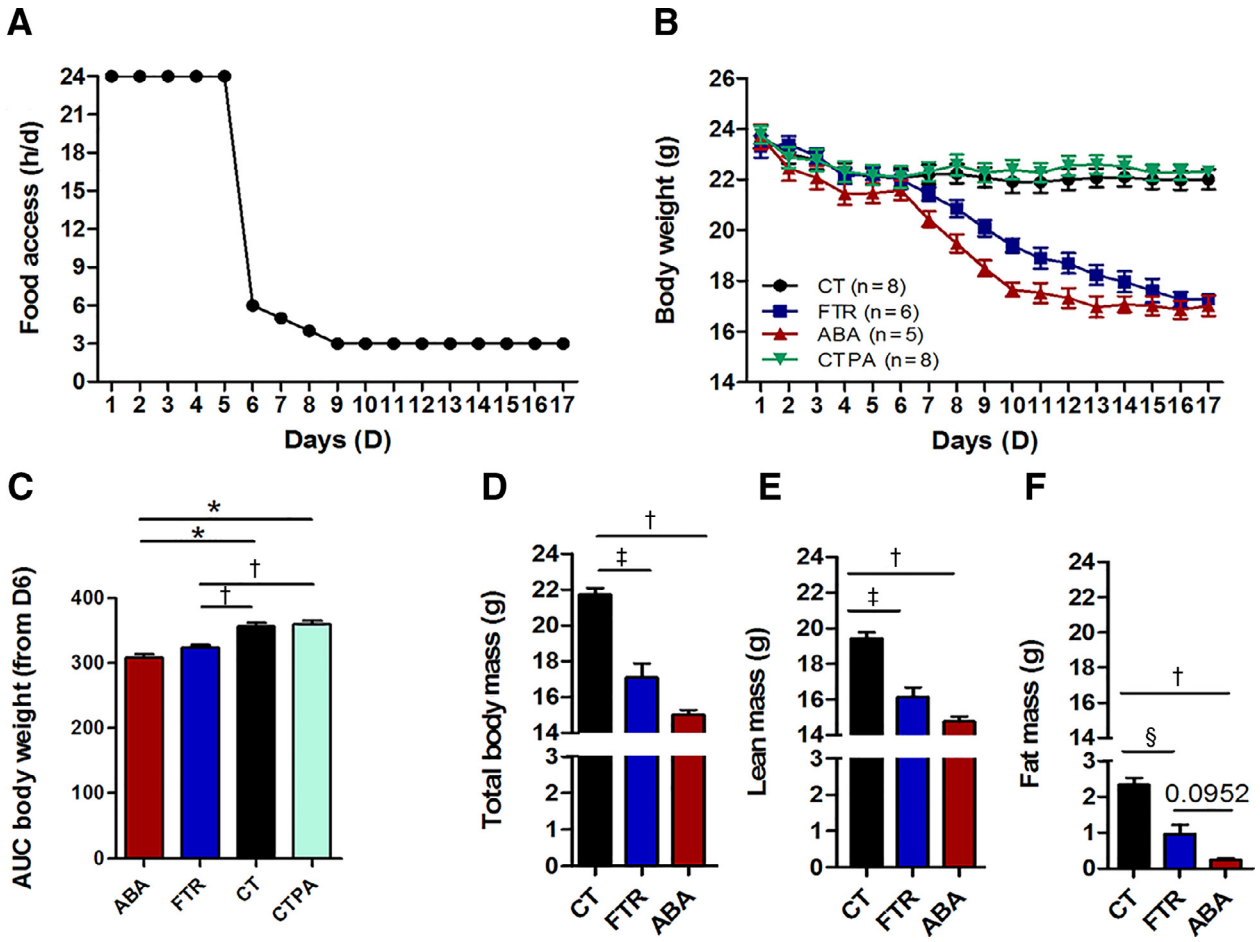

Fig. 1. Body weight and body composition. (**A**) Protocol of daily food access in ABA and FTR mice. (**B**) Daily dynamics of body weight changes. (**C**) AUC of body weight from day 6. (**D**) **t**otal tissue mass, (**E**) lean tissue mass and (**F**) fat tissue mass measured by echoMRI at day 17. (**C**) ANOVA $P < 0.0001$, Bonferroni's post-test CTPA and CT vs ABA. $^{*}P < 0.0001$, CTPA and CT vs FTR. $^{\dagger}P < 0.001$ (**D**) ANOVA $P = 0.0017$, Dunn's post-test CT vs FTR. $^{\ddagger}P < 0.05$ and CT vs ABA. ANOVA $^{\dagger}P < 0.01$. (**E**) ANOVA $P = 0.0019$, Dunn's post-test CT vs FTR. $^{\ddagger}P < 0.05$ and CT vs ABA. ANOVA $^{\dagger}P < 0.01$. (**F**) ANOVA $P = 0.0035$, Dunn's post-test CT vs ABA. $^{\dagger}P < 0.01$. $^{\ddagger}P < 0.05$ Student's *t* test CT vs FTR. $^{\S}P = 0.032$, *t* test two-tailed FTR vs ABA. $P = 0.0952$. ABA, activity-based anorexia; ANOVA, analysis of variance; AUC, area under curve; CT, Control; CTPA, control with physical activity; D6, day 6; FTR, feeding-time restriction; MRI, magnetic resonance imaging.

without activity wheel. From D1 to D5, mice had free access to water and standard diet. Food access was progressively limited in ABA and FTR groups from 6 h on D6 to 3 h on D9 until the end of experiment. Food was given at the beginning of the dark phase (0930). Food consumption was measured when food was removed. Body weight, water, and food consumption were measured daily at 0900. In the ABA and FTR groups, water and food intake also were monitored when food was removed. Experiments were carried out until D17. Mice showing excessive weight loss (>20%) over 3 d consecutively were sacrificed for ethical reasons. At D17, mice were sacrificed and pellets were collected directly in colon and immediately frozen at −80°C for further proteomic analysis of gut microbiota. Trunk blood was collected after decapitation and plasma was separated by centrifugation.

Body composition

Total, lean, and fat mass were measured in vigil mice on the last day of the experimental protocol (D17) using EchoMRI EMR-185 (EchoMRI, Houston, TX, USA), a nuclear magnetic resonance instrument.

Proteins extraction

Proteins extractions from feces were performed as described by Flores et al., with slight modifications [36]. Briefly, feces were thawed in phosphate-buffered saline then transferred to a proteins extraction buffer [urea 7 mol/L, thiourea 2 mol/L, dithiothreitol 20 mmol/L, CHAPS and tributylphosphate]. The fecal content was homogenized by vortexing for 2 min. Then, bacterial cells were lysed by sonication during 90s (Bioblock Scientific, France) before centrifugation 22 000*g* during 30 min at 4°C. Supernatants were sampled to perform ultracentrifugation at 100 000*g* for 1 h at 4°C to isolate proteins from residual debris.

Two-dimensional PAGE

For 2-D polyacrylamide gel electrophoresis (PAGE), 300 μg of fecal protein extract was used to rehydrate immobilized pH gradient (IPG) strips (pH 4.0−7.0; 18 cm; BIO-RAD, Hercules, CA, USA). Proteins were separated in the first dimension by isoelectric focusing for a total of 85 000 V-h by using the IPGphor isoelectric focusing system (GE Healthcare, Chicago, IL, USA). After focusing, IPG strips were incubated for 15 min in the equilibration buffer (urea 6 mol/L, 30% [vol:vol] glycerol, 2% [wt:vol] sodium dodecyl sulfate [SDS], Tris-HCl 50 mmol/L pH 8.8, and 0.25% [wt:vol] bromophenol blue containing 2% [wt:vol] dithiothreitol) and then alkylated for 15 min in the equilibration buffer containing 4% (wt:vol) iodoacetamide. IPG strips were subsequently fixed onto 10% polyacrylamide gradient gels (20 cm height · 18 cm width · 1 mm depth) for SDS-PAGE. Separation of proteins in second dimension according to molecular weight was performed overnight in the Ettan Daltsix vertical electrophoresis system (GE Healthcare) with 12 mA/gel at 25°C. After SDS-PAGE, the 2-D gels were fixed for 2 h in 2% (vol:vol) orthophosphoric acid and in 50% (vol:vol) methanol at room temperature. Gels were then rinsed with water, and the protein spots were visualized by CBB G-250 (BIO-RAD) staining (34% [vol:vol] methanol, 17% [wt:vol] ammonium sulfate, 2% [vol:vol] orthophosphoric acid, and 0.66 g CBB G-250/L).

Analysis of differential protein expression

Images of stained 2-D gels were scanned by an ImageScanner II (GE Healthcare) calibrated with a gray-scale marker (Kodak, Rochester, NY) and digitalized with Labscan 6.0 software (GE Healthcare). Analysis of differential protein expression including spot detection, quantification, matching, and comparative analysis was performed using Progenesis samespot software (GE Healthcare). Each protein sample was subjected to 2-D PAGE at least three times to minimize run-to-run variation, and each set of three gels was compared using Progenesis to confirm the non-appearance of statistically differential spots within the set of gels. The expression level was determined by the relative volume of each spot in the gel and expressed as percent volume, calculated as spot volume/Σvolumes of all spots resolved in the gel. This normalized spot volume takes into account variations due to protein loading and staining by considering the total volume over all the spots present in the gel. Variations in abundance were calculated as the ratio of average values of percent volume for a group of spots between the two phases. Only spots with a percent volume variation ratio >1.5 were considered relevant. The absence of a spot within a gel indicated that no detectable expression could be reported for the protein under the selected experimental condition. The corresponding *P*-values were determined by Student's *t* test (significance level $P < 0.05$) after spot percent volume log-transformation.

Protein identification by liquid chromatography-electrospray ionization MS/MS

The protein spots of interest were excised from CBB G-250-stained 2-D gels using the Ettan Spot Picker (GE Healthcare), and automated in-gel digestion of proteins was performed on the Ettan Digester (GE Healthcare). Protein extracts were then resuspended in 10 μL of 5% (vol:vol) acetonitrile/0.1% (vol:vol) formic acid and then analyzed with a nano-LC1200 system coupled to a 6340 Ion Trap mass spectrometer equipped with a nanospray source and an high-performance liquid chromatography-chip cube interface (Agilent Technologies, Les Ulis, France). Briefly, peptides were enriched and desalted on a 40 nL RP-C18 trap column and separated on a Zorbax (30-nm pore size, 5-μm particle size) C18 column (43 mm long × 75 μm inner diameter; Agilent Technologies). A 9-min linear gradient (3−80% acetonitrile in 0.1% formic acid) at a flow rate of 400 nL/min was used and the eluent was analyzed with an ion trap mass spectrometer (MS).

For protein identification, MS/MS peak lists were extracted and compared with the protein databases by using the MASCOT Daemon version 2.2.2 (Matrix Science) search engine. The searches were performed with the following specific parameters: enzyme specificity, trypsin; one missed cleavage permitted; no fixed modifications; variable modifications, methionine oxidation, cysteine carbamidomethylation, serine, tyrosine and threonine phosphorylation; monoisotopic; peptide charge, 2+ and 3+; mass tolerance for precursor ions, 1.5 Da; mass tolerance for fragment ions, 0.6 Da; ESI-TRAP as instrument; taxonomy, bacteria; National Center for Biotechnology Information (NCBI) database (NCBInr 20120531 [18280215 sequences, 6265275233 residues]; Bethesda, MD, UA). Protein hits were automatically validated if they satisfied one of the following criteria: identification with at least two top-ranking peptides (bold and red) each with a MASCOT score of >54 ($P < 0.01$), or at least two top-ranking peptides (bold and red) each with a MASCOT score of >47 ($P < 0.05$). To evaluate false-positive rates, all the initial database searches were performed using the "decoy" option of MASCOT. Results were considered relevant if the false-positive rate never exceeded 1%.

ATP assay

In vitro ATP production was measured using ATP colorimetric/fluorometric assay kit according to the manufacturer's instructions (BioVision, CA, USA). Briefly, bacterial proteins from feces of ABA, CT, FTR, and CTPA mice were put in duplicates into the wells at 1 μg/μL concentration in ATP assay buffer and adjusted to 40 μL/well with ATP assay buffer. Then, 10 μL of nutrients solution MH culture medium were added; MH medium contains 30% beef infusion, 1.75% casein hydrolysate, and

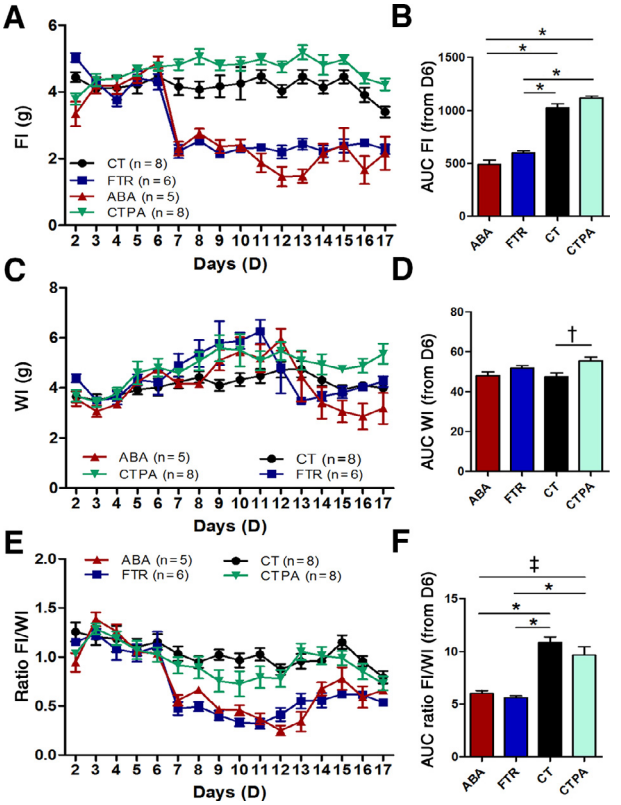

Fig. 2. Food and water intakes. (**A**) Dynamics of daily FI (**B**) AUC from D6 of food intake. (**C**) Dynamics of daily WI (**D**) AUC form D6 of WI. (**E**) Dynamics of daily ratios of FI and WI (**F**) AUC from D6 of FI/WI ratios. (**B**) ANOVA $P < 0.0001$, Bonferroni's post-test CTPA. and CT vs ABA and FTR, $^{*}P < 0.0001$. (**D**) ANOVA $P = 0.0214$, Bonferroni's post-test CT vs CTPA, $^{\dagger}P < 0.05$. (**F**) ANOVA $P < 0.0001$, Bonferroni's post-test CTPA and CT vs FTR, CT vs ABA $^{*}P < 0.0001$, CTPA vs ABA $^{\ddagger}P < 0.01$. ABA, activity-based anorexia; ANOVA, analysis of variance; AUC, area under curve; CT, control; CTPA, control with physical activity; D6, day 6; FI, food intake; FTR, feeding-time restriction; WI, water intake.

0.15% starch (Becton Dickinson, Baltimore, MD, USA). The plate was incubated for 2 h at 37°C. After the incubation, 50 μL of ATP reaction mix (containing ATP assay buffer, ATP probes, ATP converter, and developer mix) were added in each wells. Optical density was measured at 570 nm after 30 min of incubation at room temperature, protected from day light.

Acetate assay

In vitro acetate production was measured using an Acetate Colorimetric Assay kit according to the manufacturer's instructions (Sigma-Aldrich, St. Louis, MO, USA). Briefly, plasma from ABA, CT, FTR and CTPA was placed into the plate with 50 μL per well. After the incubation, 50 μL of acetate reaction mix (containing acetate assay buffer, probes, ATP, acetate enzyme, and acetate substrate mix) were added to each well. Optical Density (O.D.) was measured at 450 nm after 40 min of incubation at room temperature, protected from day light.

Statistical analysis

Data were analyzed and graphs were plotted using the GraphPad Prism 5.02 (GraphPad Software Inc., San Diego, CA, USA). Normality was evaluated by the Kolmogorov–Smirnov test. Group differences were analyzed by the analysis of variance (ANOVA) or the non-parametric Kruskal–Wallis (K–W) test with the Tukey's or Dunn's post-tests, according to the normality results. Where appropriate, individual groups were compared using the Student's t test or the Mann–Whitney (M–W) test according to the normality results. Data are shown as means ± SEM, and for all test, $P < 0.05$ was considered statistically significant.

Results

Body weight and body composition

In response to food restriction, both FTR and ABA mice showed a significant decrease of body weight as compared to the sedentary control group (CT) and control mice with free access to a running wheel (CTPA). At the beginning of the feeding time restriction (D6–12), body weight loss was more pronounced in ABA than in FTR mice, but the final weight loss was similar at the end of the experiment (Fig. 1B, C). Analysis of body composition revealed a decrease of total, lean, and fat mass in both groups of food-restricted mice (Fig. 1D–F). However, the decrease of fat mass in ABA mice was more pronounced than in the FTR group (Fig. 1F).

Food and water intake

As expected, during the food-restriction period, food intake in both ABA and FTR mice was lower than in ad libitum-fed groups but it was not significantly different between the ABA and FTR groups (Fig. 2A, B). Water intake was not significantly different in food restricted versus sedentary controls, whereas the CTPA group displayed higher water intake (Fig. 2C, D). Both ABA and FTR mice showed a decrease in food intake/water intake ratios during the food-restriction period compared with CT and CTPA groups (Fig. 1E, F).

Physical activity

ABA mice showed a transitory increase of physical activity during food restriction from D7 to D9 followed by a progressive decline of total activity toward the end of the protocol (Fig. 3A). In CTPA mice, physical activity occurred only in the dark phase; whereas in ABA mice it was mainly in the dark phase but some activity was also present in the light phase, which was due to feeding anticipatory activity (Fig. 3A versus B). Indeed, the analysis of physical activity (from D8 to D17) during 3 h preceding food provision showed a

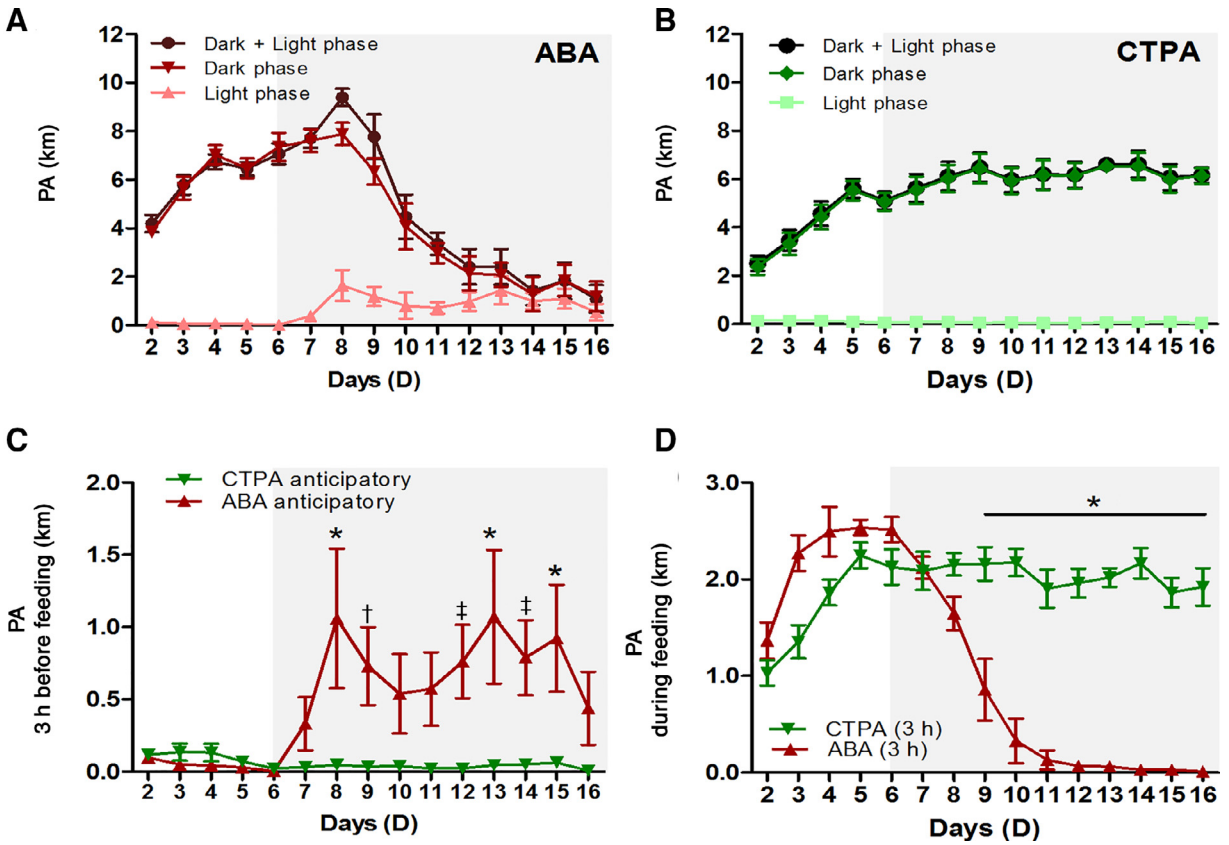

Fig. 3. Physical activity. (**A**) Daily PA (running distance in km) in ABA mice and in CTPA mice (**B**). (**C**) Feeding anticipatory activity 3 h before food access and PA during 3 h of feeding period (**D**) in ABA and CTPA mice. (**C**) Two-way ANOVA, Bonferroni's post-test ABA vs CTPA, D8, D13, D15 $^{*}P < 0.0001$; D12, D14 $^{‡}P < 0.01$; D9 $^{†}P < 0.05$ (**D**) Two-way ANOVA, Bonferroni's post-test ABA vs CTPA., from D9 to D16, $^{*}P < 0.0001$. ABA, activity-based anorexia; ANOVA, analysis of variance; CTPA, control with physical activity; D, day; PA, physical activity.

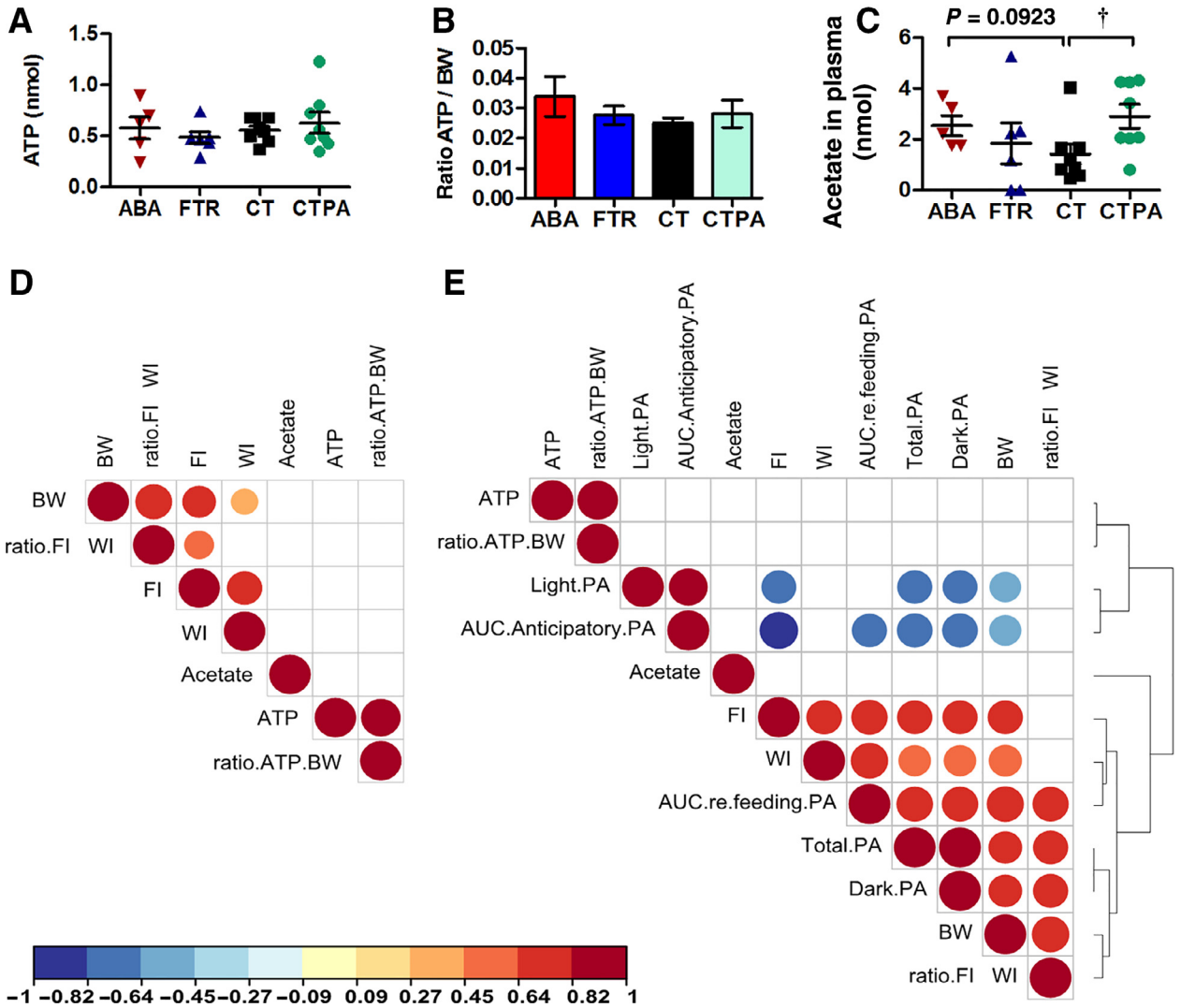

Fig. 4. ATP production by bacterial proteins from feces. (**A**) In vitro assay of ATP production by gut bacterial proteins extracted from feces of ABA, FTR, CT, and CTPA mice. (**B**) ATP production relative to body weight of mice. (**C**) Acetate plasma concentration in ABA, FTR, CT, and CTPA mice. (**D**) Correlations of study parameters in all groups. (**E**) Correlations of study parameters including physical activity in ABA and CTPA groups. Circles denote significant ($P < 0.05$) negative (blue) and positive (red) Spearman's correlations. (**C**) †$P = 0.032$, *t* test two-tailed CT vs CTPA. ABA, activity-based anorexia; ATP, adenosine triphosphate; BW, body weight; CT, control; CTPA, control with physical activity; FI, food intake; FTR, feeding-time restriction; WI, water intake.

significant increase in ABA mice (Fig. 3C). During feeding periods, ABA mice progressively decreased their physical activity showing an adaptation to the feeding time-restriction schedule (Fig. 3D).

ATP production by bacterial proteins from feces

To analyze whether the capacity of bacterial proteins to produce ATP is altered in starved mice, we incubated in vitro for 2 h total proteins from feces of ABA, FTR, CT, and CTPA mice with MH culture medium (as a source of nutrient) and measured ATP concentration in the incubation medium. No significant difference of in vitro ATP production by bacterial proteins was found between the groups (Fig. 4A). Adjustment of ATP production by body weight of mice did not result in significant differences between the groups either (Fig. 4B).

Plasma acetate and correlations between biological parameters

Acetate is one of the end products of carbohydrate fermentation by colonic microbiota and is an alternative source of energy for the brain [37]. Because acetate also has been shown to induce anorexigenic effect in the brain [38], we measured acetate plasma concentrations in mice on D17. We found that plasma acetate was higher in the group of mice with physical activity (CTPA) and tended to be higher in ABA mice (*t* test two-tailed $P = 0.094$) compared with CT mice (Fig. 4C).

To gain further insight into the possible links between the biological parameters assayed in the present study, they were compared by correlation analysis. As illustrated by the correlograms no significant correlations were found between ATP-production capacity or plasma acetate with behavioral parameters either in all groups (Fig. 4D) or in groups of mice with physical activity (Fig. 4E). Significant negative correlations were found between the feeding anticipatory activity and food intake and body weight, indicating that such physical activity was a contributor to the weight loss in the ABA group. Conversely, as expected, food and water intakes correlated positively with body weight (Fig. 4D, E)

Proteomic analysis of feces

2-D electrophoresis gels were run using total proteins samples extracted from feces collected from the colon of the CT, FTR, and

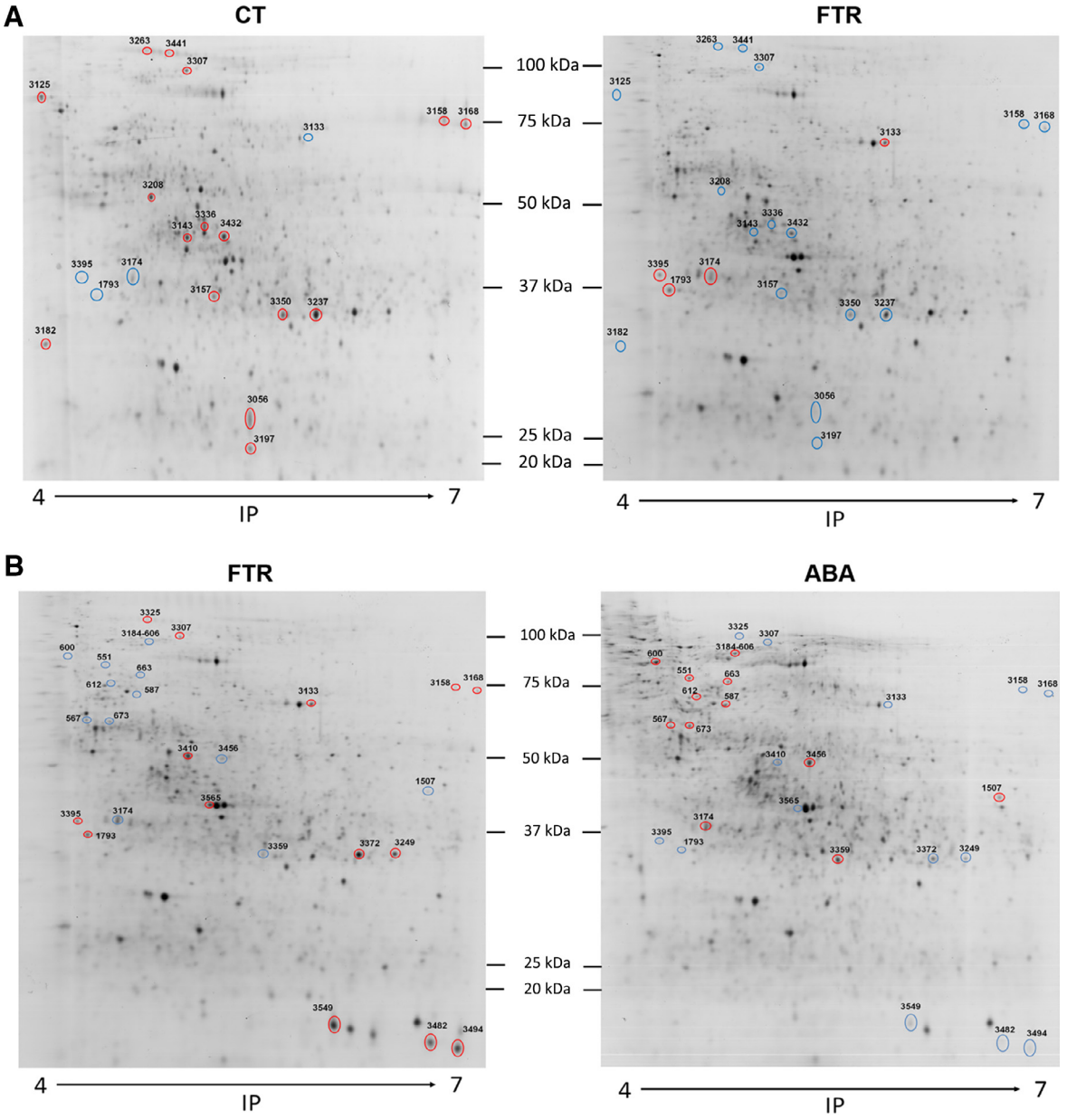

Fig. 5. Representative images of Coomassie-stained two-dimensional gels of fecal proteins. (**A**) CT vs FTR and (**B**) FTR vs ABA. Differentially expressed proteins (i.e., with ≥1.5-fold change, Student's *t* test, $P < 0.05$) are shown as encircled spots. Red = increase, blue = decrease. ABA, activity-based anorexia; CT, control; FTR, feeding-time restriction; IP, isoelectric point.

ABA groups on D17 (Fig. 5). After comparison of proteome profiles we found that 20 protein spots were differentially expressed between CT and FTR groups. Among them, 16 proteins were overexpressed in the CT group, whereas only 4 were overexpressed in the FTR group (Fig. 5A). Moreover, 26 protein spots were found to be differentially expressed between the FTR and ABA groups. Among them, 14 were overexpressed in the FTR group and 12 were overexpressed in the ABA group (Fig. 5B). Some, but not all differentially expressed proteins have been identified by MS. The results of the identification are presented in Table 1. Of note, increased levels of the phosphoglycerate kinase, an ATP-producing glycolytic enzyme belonging to the *Clostridium* sp. ASF502, were detected in the feces of FTR mice and this enzyme was further increased in the ABA group. Starvation also upregulated several other proteins from the *Clostridium* sp. ASF502 and from *Lachnospiraceae* family, both belonging to the *Clostridiales* order.

Discussion

In the present study, we analyzed gut bacterial proteome in chronically starved mice using behavioral models with limited access to food with or without physical activity in a running wheel (i.e., in the ABA and FTR groups, respectively). The validity of the experimental approach was confirmed by significant loss of body weight and decrease of food and water intake in both the ABA and FTR groups. The limitation of this model is that such "anorexia" will disappear as soon as the animals will have ad libitum access to food. In the present experiment, mice in the ABA group did not, for the majority, display lower food intake than the FTR group, apart from few sporadic decreases (Fig. 2A). Nevertheless, lower levels of fat mass and a more significant loss of total body mass than in FTR group show a greater degree of starvation in the ABA group. This starvation was due to both a decrease of food intake and increased

Table 1
Identified bacterial proteins in feces of mice*

Spot	NCBI nr accession number	Protein name	Bacterial clades	IP	MW (Da)	Cover (%)	Fold changes
CT group							
3056	gi 393783424	Hypothetical protein HMPREF1071_02465	*Bacteroidales (Bacteroidaceae, Bacteroidetes salyersiae CT02 T12 CO1)*	5.44	**72169**	**7**	**2.8 vs FTR**
3125	gi 46909475	Flagellin (uncultured bacterium)	*Unknown*	5.05	**48935**	**9**	**4.8 vs FTR**
3143	gi 255283697	Translation elongation factor Tu	*Clostridiales (Clostridiaceae, Bryantella formatexigen DSM 14469)*	5.04	**43815**	**32**	**3.6 vs FTR**
FTR group							
1793	gi 302669857	Flagellin Flic1	*Clostridiales (Lachnospiraceae, Butyrivibrio proteoclasticus B316)*	5.3	**31337**	**14**	**2.4 vs CT/ABA**
3174	gi 476628170	Phosphoglycerate kinase	*Clostridiales (Clostridiaceae, Clostridium sp ASF502)*	4.93	**41780**	**22**	**1.8 vs CT**
3410	gi 336430440	Elongation factor Tu	*Clostridiales (Lachnospiraceae bacterium 3157 FAA CT1)*	5.05	**43928**	**6**	**3.6 vs ABA**
ABA group							
663	gi 490181412	Hypothetical protein	*Clostridiales (Clostridiaceae, Clostridium sp ASF502)*	4.92	**89955**	**27**	**2.9 vs FTR**
673	gi 496554534	UDP kinase	*Clostridiales (Lachnospiraceae bacterium 7_1_58 FAA)*	5.42	**42664**	**14**	**2.6 vs FTR**
1507	gi 490173254	Hypothetical protein	*Clostridiales (Clostridiaceae, Clostridium sp ASF502)*	7.03	**29270**	**29**	**2.5 vs FTR**
3174	gi 490169794	Phosphoglycerate kinase	*Clostridiales (Clostridiaceae, Clostridium sp ASF502)*	4.93	**41780**	**25**	**1.8 vs FTR**
3359	gi 490169796	Gyceraldehyde-3-phosphate dehydrogenase	*Clostridiales (Clostridiaceae, Clostridium sp ASF502)*	5.1	**35913**	**29**	**2.63 vs FTR**

ABA, activity-based anorexia; CT, control; FTR, feeding-time restriction.
*Differentially expressed proteins (i.e., with at least 1.5-fold change, Student's *t* test, $P < 0.05$), which were identified by liquid chromatography-tandem mass spectrometry in CT, FTR, and ABA groups.

anticipatory physical activity supported by significant correlations with body weight of both parameters. Weight loss was not related to dehydration because no decrease in water intake was observed resulting in lower ratios of food to water intakes in either the ABA or the FTR groups. We also observed that during starvation, mice adapted to the restricted feeding more often by reducing physical activity than by increasing food intake [30]. Because we used male mice, which we previously found to be more susceptible to developing ABA, these data are in agreement with results showing reduced plasticity of hippocampal GABA-ergic neurons in male mice contributing to the development of ABA [39]. Although AN is predominantly a female pathology, the sex ratio tends to evolve over the time, suggesting that AN pathology could be also a male concern [40].

Starvation creates an energy deficit for the body including the brain, which consumes about 20% of oxygen and 25% of glucose. It has been estimated that glutamate-mediated neurotransmission is responsible for most (~80%) of the energy expenditure in the gray matter [41]. Neurons receive their energy substrates mainly in the form of lactate from astrocytes, which are highly glycolytic [42]. This is relevant to AN because reduced astrocyte density was observed in animals with ABA [43], possibly underlying the loss of brain volume in patients with AN [44]. Also, ABA mice exhibit brain modifications of hypothalamic proteins mainly involved in energy metabolism such as glycolysis and tricarboxylic acid cycle [45]. To meet the demands of the host, gut bacteria could represent an alternative source of energy substrates for the body and the brain due to the capacity of bacterial enzymes to catalyze production of ATP, lactate, and SCFA such as acetate, butyrate, and propionate, which pass from the gut to the systemic circulation [38]. The present results revealed modifications of the bacterial proteome in feces of starved mice by showing an upregulation of several glycolytic enzymes including phosphoglycerate kinase (PGK), a major ATP-producing glycolytic enzyme [46].

In the present study, the proteomic investigations of the fecal/colonic microbiota could represent a limit because the main place of the fermentation is located in the caecum. However, the specific fecal/colonic microbiota may be of interest since increased colonic permeability characterized the ABA mice [47], which could lead to gut microbiota modifications. Also, a specific fecal microbiota profile has been found to be significantly different from the cecal one with biological and functional relevance regarding the bacterial catabolism [48]. It is also worth noting that the proteins identified in this study (and assigned to *Clostridium* sp ASF502) could match with other bacteria either from the *Lachnospiraceae* family or from the *Clostridiaceae* family both belonging to the order *Clostridiales*. Of notice, the PGK belonged to the order *Clostridiales* and it was further upregulated in ABA compared with the FTR mice, suggesting that PGK levels can be linked to the starvation degree. This finding supports the idea that starvation-induced increase of the PGK expression by selective gut bacteria may provide an additional tool for the ATP supply for the body to combat energy deficit. Another glycolytic enzyme, the glyceraldehyde 3-phosphate dehydrogenase (GAPDH) produced by *Clostridium* was found to be upregulated in the fecal proteome of ABA mice. GAPDH precedes PGK in the glycolysis metabolic pathway and generates energy by producing nicotinamide adenine dinucleotide. The fecal microbiota of ABA mice seems to produce energy substrates with a greatest efficacy than the fecal microbiota of CT mice. Also, an upregulation of glycolytic enzymes (such as PGK) can be the result of utilization of substrates from lipolysis and glycerol metabolism for the host.

Despite increased levels of the *Clostridium* PGK detected by proteomics, our in vitro assay of gut bacterial enzyme activity did not show differences in ATP production between starved and ad libitum-fed mice. These results suggest that the capacities of bacterial ATP production are limited to the maintenance of normal levels of ATP synthesis during starvation, which may partly compensate for eventual losses of ATP and other energy substrate production after modification of the microbiome composition. In fact, several studies revealed low levels of SCFA in feces of patients with AN [6,8,9]. This may reflect a decrease of SCFA-producing bacterial species in AN such as *Roseburia* (family *Lachnospiraceae*, order *Clostridiales*), which abundance correlates with butyrate [8,9]. A decrease of SCFA production by gut bacteria is of functional relevance as SCFA

may account for ≤10% of the energy substrate supply [49]. In the present study, we measured plasma levels of acetate, which tended to be higher in ABA versus CT mice. However, it was not increased in the FTR mice, suggesting that it was not primarily linked to starvation, but rather to physical activity because ad libitum-fed running mice also displayed significant elevated plasma acetate.

It is of interest that all the identified proteins, which were upregulated in both ABA and FTR mice, belonged to the order *Clostridiales* (Table 1). In fact, beside the glycolytic enzymes, increased expression of uridine diphosphate (UDP) kinase and of the elongation factor Tu both produced of *Lachnospiraceae* bacterium were detected in the ABA and FTR mice, respectively. Flagellin, a structural protein from a butyrate-producing bacterium *Butyrivibrio proteoclasticus* (family *Lachnospiraceae*, order *Clostridiales*) was also increased in the FTR mice. Taken together, these data point to increased metabolic activities of *Clostridiales* during starvation. Increased abundance of *Clostridiales* also has been found in the ABA model in rats correlating negatively with plasma leptin [34]. Thus, although the ABA model in rodents can only partly reflect chronic starvation in patients with AN, the present data support a role of the order *Clostridiales* in the adaptation of gut microbiota to host starvation via increased capacity in energy harvesting to produce energy substrates and maintain ATP synthesis.

References

[1] Fairburn CG, Harrison PJ. Eating disorders. Lancet 2003;361:407–16.
[2] Fetissov SO. Role of the gut microbiota in host appetite control: bacterial growth to animal feeding behaviour. Nat Rev Endocrinol 2017;13:11–25.
[3] Cryan JF, Dinan TG. Mind-altering microorganisms: the impact of the gut microbiota on brain and behaviour. Nat Rev Neurosci 2012;13:701–12.
[4] Cani PD, Knauf C. How gut microbes talk to organs: the role of endocrine and nervous routes. Molecular Metabolism 2016;5:743–52.
[5] Armougom F, Henry M, Vialettes A, Raccah D, Raoult D. Monitoring bacterial community of human gut microbiota reveals an increase in lactobacillus in obese patients and methanogens in anorexic patients. PLoS One 2009;4:e7125.
[6] Morita C, Tsuji H, Hata T, Gondo M, Takakura S, Kawai K, et al. Gut dysbiosis in patients with anorexia nervosa. PLoS One 2015;10:e0145274.
[7] Kleiman SC, Watson HJ, Bulik-Sullivan EC, Huh EY, Tarantio LM, Bulik CM, et al. The intestinal microbiota in acute anorexia nervosa and during renourishment: relationship to depression, anxiety, and eating disorder psychopathology. Psychosom Med 2015;77:969–81.
[8] Mack I, Cuntz U, Gramer C, Niedermaier S, Pohl C, Scheiertz A, et al. Weight gain in anorexia nervosa does not ameliorate the faecal microbiota, branched chain fatty acid profiles, and gastrointestinal complaints. Sci Rep 2016;6:26752.
[9] Borgo F, Riva A, Benetti A, Casiraghi MC, Bertelli S, Garbossa S, et al. Microbiota in anorexia nervosa: the triangle between bacterial species, metabolites and psychological tests. PLoS One 2017;12:e0179739.
[10] Mörkl S, Lackner S, Muller W, Gorkiewicz G, Kashofer K, Oberascher A, et al. Gut microbiota and body composition in anorexia nervosa inpatients in comparison to athletes, overweight, obese, and normal weight controls. International J Eat Disord 2017;50:1421–31.
[11] Herpertz-Dahlmann B, Seitz J, Baines J. Food matters: how the microbiome and gut–brain interaction might impact the development and course of anorexia nervosa. Eur Child Adolesc Psychiatry 2017;26:1031–41.
[12] Glenny EM, Bulik-Sullivan EC, Tang Q, Bulik CM, Carroll IM. Eating disorders and the intestinal microbiota: mechanisms of energy homeostasis and behavioral influence. Curr Psychiatry Rep 2017;19:51.
[13] Karakula-Juchnowicz H, Pankowicz H, Juchnowicz D, Valverde Piedra JL, Malecka-Massalska T. Intestinal microbiota – a key to understanding the pathophysiology of anorexia nervosa? Psychiatr Pol 2017;51:859–70.
[14] Lam Y, Maguire S, Palacios T, Caterson ID. Are the gut bacteria telling us to eat or not to eat? Reviewing the role of gut microbiota in the etiology, disease progression and treatment of eating disorders. Nutrients 2017;9:602.
[15] Schwensen HF, Kan C, Treasure J, Hoiby N, Sjogren M. A systematic review of studies on the faecal microbiota in anorexia nervosa: future research may need to include microbiota from the small intestine. Eat Weight Disord 2018;23:399–418.
[16] Mack I, Penders J, Cook J, Dugmore J, Mazurak N, Enck P. Is the impact of starvation on the gut microbiota specific or unspecific to anorexia nervosa? A narrative review based on a systematic literature search. Curr Neuropharmacol 2018;16:1131–49.
[17] Russell JB, Cook GM. Energetics of bacterial growth: balance of anabolic and catabolic reactions. Microbiol Rev 1995;59:48–62.
[18] Canfora EE, Jocken JW, Blaak EE. Short-chain fatty acids in control of body weight and insulin sensitivity. Nat Rev Endocrinol 2015;11:577–91.
[19] LeBlanc JG, et al. Beneficial effects on host energy metabolism of short-chain fatty acids and vitamins produced by commensal and probiotic bacteria. Microbial Cell Factories 2017;16:79.
[20] Breton J, Tennoune N, Lucas N, Francois M, Legrand R, Jacquemot J, et al. Gut commensal E.coli proteins activate host satiety pathways following nutrient-induced bacterial growth. Cell Metab 2016;23:1–11.
[21] Routtenberg A, Kuznesof AW. Self-starvation of rats living in activity wheels on a restricted feeding schedule. J Comp Physiol Psychol 1967;64:414–21.
[22] Carrera O, Fraga A, Pellon R, Gutierrez E. Rodent model of activity-based anorexia. Curr Protoc Neurosci 2014;67. 9.47.1–11.
[23] Chudecka M, Lubkowska A. Thermal imaging of body surface temperature distribution in women with anorexia nervosa. Eur Eat Disord Rev 2016;24:57–61.
[24] Pare WP. Body temperature and the activity-stress ulcer in the rat. Physiol Behav 1977;18:219–23.
[25] Warren MP. Vande Wiele RL Clinical and metabolic features of anorexia nervosa. Am J Obstet Gynecol 1973;117:435–49.
[26] Tchanturia K, Davies H, Harrison A, Fox JR, Treasure J, Schmidt U. Altered social hedonic processing in eating disorders. Int J Eat Disord 2012;45:962–9.
[27] Verty AN, Evetts MJ, Crouch GJ, McGregor IS, Stefanidis A, Oldfield BJ. The cannabinoid receptor agonist THC attenuates weight loss in a rodent model of activity-based anorexia. Neuropsychopharmacology 2011;36:1349–58.
[28] Pare WP. The influence of food consumption and running activity on the activity-stress ulcer in the rat. Am J Dig Dis 1975;20:262–73.
[29] Zipfel SGiel KE, Bulik CM, Hay P, Schmidt U. Anorexia nervosa: aetiology, assessment, and treatment. Lancet Psychiatry 2015;2:1099–111.
[30] Achamrah N, Nobis S, Goichon A, Breton J, Legrand R, do Rego JL, et al. Sex differences in response to activity-based anorexia model in C57Bl/6 mice. Physiol Behav 2017;170:1–5.
[31] Davis C, Katzman DK, Kaptein S, Kirsh C, Brewer H, Kalmbach K, et al. The prevalence of high-level exercise in the eating disorders: etiological implications. Compr Psychiatry 1997;38:321–6.
[32] Pjetri E, de Haas R, de Jong S, Gelegen C, Oppelaar H, Verhagen LA, et al. Identifying predictors of activity based anorexia susceptibility in diverse genetic rodent populations. PLoS One 2012;7:e50453.
[33] Lamanna J, Sulpizio S, Ferro M, Martoni R, Abutalebi J, Malgaroli A. Behavioral assessment of activity-based-anorexia: how cognition can become the drive wheel. Physiol Behav 2019;202:1–7.
[34] Queipo-Ortuno MI, Seoane LM, Murri M, Pardo M, Gomez-Zumaquero JM, Cardona F, et al. Gut microbiota composition in male rat models under different nutritional status and physical activity and its association with serum leptin and ghrelin levels. PLoS One 2013;8:e65465.
[35] Achamrah N, Nobis S, Breton J, Jesus P, Belmonte L, Maurer B, et al. Maintaining physical activity during refeeding improves body composition, intestinal hyperpermeability and behavior in anorectic mice. Sci Rep 2016;6:21887.
[36] Flores R, Shi J, Gail MH, Ravel J, Goedert JJ. Assessment of the human faecal microbiota: I. Measurement and reproducibility of selected enzymatic activities. Eur J Clin Invest 2012;42:848–54.
[37] Andersen JV, McNair LF, Schousboe A, Waagepetersen HS. Specificity of exogenous acetate and glutamate as astrocyte substrates examined in acute brain slices from female mice using methionine sulfoximine (MSO) to inhibit glutamine synthesis. J Neurosci Res 2017;95:2207–16.
[38] Frost G, Sleeth ML, Sahuri-Arisoylu M, Lizarbe B, Cerdan S, Brody L, et al. The short-chain fatty acid acetate reduces appetite via a central homeostatic mechanism. Nat Commun 2014;5:3611.
[39] Chen YW, Actor-Engel H, Aoki C. α4-GABAA receptors of hippocampal pyramidal neurons are associated with resilience against activity-based anorexia for adolescent female mice but not for males. Mol Cell Neurosci 2018;90:33–48.
[40] Galmiche M, Dechelotte P, Lambert G, Pierre Tavolacci M. Prevalence of eating disorders over the 2000–2018 period: a systematic literature review. Am J Clin Nutr 2019;109:1402–13.
[41] Bélanger M, Allaman I, Magistretti PJ. Brain energy metabolism: focus on astrocyte-neuron metabolic cooperation. Cell Metab 2011;14:724–38.
[42] Pellerin L, Magistretti PJ. Glutamate uptake into astrocytes stimulates aerobic glycolysis: a mechanism coupling neuronal activity to glucose utilization. Proc Natl Acad Sci 1994;91:10625–9.
[43] Frintrop L, Liesbrock J, Paulukat L, Johann S, Kas MJ, Tolba R, et al. Reduced astrocyte density underlying brain volume reduction in activity-based anorexia rats. World J Biol Psychiatry 2018;19:225–35.
[44] Seitz J, Herpertz-Dahlmann B, Konrad K. Brain morphological changes in adolescent and adult patients with anorexia nervosa. J Neural Transm 2016;123:949–59.
[45] Nobis S, Goichon A, Achamrah N, Guerin C, Azhar S, Chan P, et al. Alterations of proteome, mitochondrial dynamic and autophagy in the hypothalamus during activity-based anorexia. Sci Rep 2018;8:7233.
[46] Blake CCF, Rice DW. Phosphoglycerate kinase. Philos Trans R Soc Lond B Biol Sci 1981;293:93–104.
[47] Jésus P, Ouelaa W, Francois M, Riachy L, Guerin C, Aziz M, Do Rego JC, et al. Alteration of intestinal barrier function during activity-based anorexia in mice. Clin Nutr 2014;33:1046–53.
[48] Tanca A, Manghina V, Fraumene C, Palomba A, Abbondio M, Deligios M, et al. Metaproteogenomics reveals taxonomic and functional changes between cecal and fecal microbiota in mouse. Front Microbiol 2017;8:391.
[49] Bergman EN. Energy contributions of volatile fatty acids from the gastrointestinal tract in various species. Physiologic Rev 1990;70:567–90.